Biochemical and Biophysical Research Communications 396 (2010) 999–1005

Contents lists available at ScienceDirect

Biochemical and Biophysical Research Communications

journal homepage: www.elsevier.com/locate/ybbrc

Ultraviolet irradiation induces autofluorescence enhancement via production of reactive oxygen species and photodecomposition in erythrocytes

Xian Wu, Leiting Pan *, Zhenhua Wang, Xiaoli Liu, Dan Zhao, Xinzheng Zhang, Romano A. Rupp, Jingjun Xu **

The Key Laboratory of Weak-Light Nonlinear Photonics, Ministry of Education, TEDA Applied Physics School and School of Physics, Nankai University, Tianjin 300457, China

ARTICLE INFO

Article history:
Received 3 May 2010
Available online 13 May 2010

Keywords:
Ultraviolet irradiation
Autofluorescence
Reactive oxygen species
Photodecomposition
Erythrocytes
Rate equation

ABSTRACT

Ultraviolet (UV) light has a significant influence on human health. In this study, human erythrocytes were exposed to UV light to investigate the effects of UV irradiation (UVI) on autofluorescence. Our results showed that high-dose continuous UVI enhanced erythrocyte autofluorescence, whereas low-dose pulsed UVI alone did not have this effect. Further, we found that H_2O_2, one type of reactive oxygen species (ROS), accelerated autofluorescence enhancement under both continuous and pulsed UVI. In contrast, continuous and pulsed visible light did not result in erythrocyte autofluorescence enhancement in the presence or absence of H_2O_2. Moreover, NAD(P)H had little effect on UVI-induced autofluorescence enhancement. From these studies, we conclude that UVI-induced erythrocyte autofluorescence enhancement via both UVI-dependent ROS production and photodecomposition. Finally, we present a theoretical study of this autofluorescence enhancement using a rate equation model. Notably, the results of this theoretical simulation agree well with the experimental data further supporting our conclusion that UVI plays two roles in the autofluorescence enhancement process.

1. Introduction

In addition to infrared and visible light, solar radiation contains about 9% ultraviolet (UV) light. Although a proper dose of UV radiation is used for treatment of certain diseases, such as eosinophilic fascitis [1], cystic fibrosis, and short bowel syndrome [2]. UV radiation is generally detrimental to human health [3]. The reduction of ozone in the stratosphere has caused fears that progressively more UV radiation will reach the ground and may cause skin cancer [4,5], cataracts [5], and immune response [6]. Several factors play an important role in UV irradiation (UVI)-induced cellular physiological and pathological responses, especially reactive oxygen species (ROS), which include superoxide, hydrogen peroxide (H_2O_2) and hydroxyl radicals [7–9].

As the skin cannot entirely prevent UV radiation from penetrating to the blood supply, erythrocytes can be affected by UV light [10]. Hemoglobin [11] and the cell membrane [12] are the main targets of UV-A irradiation (315–400 nm) in erythrocytes. Erythrocytes play a key role in human metabolism, and it is therefore important to fully understand the impact of UVI on them [13]. In addition, erythrocytes often serve as model cells *in vitro* for the study of photodynamic therapy (PDT), which is an emerging new procedure for treating certain types of cancer. It has been reported [14,15] that UV-A irradiation results in strong autofluorescence in erythrocytes under PDT conditions. However, the detailed mechanisms of this UVI-induced autofluorescence enhancement are still not clear. Given this gap in the literature, the aim of this study was to investigate the relationships among UVI, PDT, ROS, photodecomposition of hemoglobin, and NAD(P)H [hydrogenated znicotinamide adenine dinucleotide (phosphate)] in human erythrocytes. In addition, we sought to theoretically analyze the photodynamic process of high-dose continuous UVI-induced autofluorescence enhancement using a rate equation model.

2. Materials and methods

2.1. Reagents

All compounds, dehydroepiandrosterone (DHEA), 2-deoxy-glucose (2-DG), trypan blue, Histopaque 1119 solution and Bovine hemoglobin were obtained from Sigma–Aldrich (St. Louis, MO, USA). All solutions were made with ultrapure water.

2.2. Isolation of erythrocytes

Human erythrocytes were obtained from the peripheral blood of healthy individuals using step density gradient centrifugation over Histopaque 1119 solutions at 500*g* for 10 min. The cells were more than 99% viable as determined by trypan blue exclusion. Isolated erythrocytes were suspended in Hanks' Balanced Salt Solu-

* Corresponding author. Fax: +86 22 66229310.
** Corresponding author. Fax: +86 22 23501743.
E-mail addresses: plt@nankai.edu.cn (L. Pan), jjxu@nankai.edu.cn (J. Xu).

0006-291X/$ - see front matter © 2010 Elsevier Inc. All rights reserved.
doi:10.1016/j.bbrc.2010.05.044

tion (HBSS) (145 mM NaCl, 5 mM KCl, 1 mM $CaCl_2$, 1 mM $MgCl_2$, 10 mM Hepes and 10 mM glucose, pH adjusted to 7.4 using 1 mM NaOH) and then kept in an ice bath before use.

2.3. Imaging system

For all imaging experiments, erythrocytes were observed at 37 °C via a temperature controlled stage. Observations were performed with a fluorescence microscope (Axio observer D1, Carl Zeiss, Germany). A shutter behind the mercury lamp was used to control the irradiation and interval times for pulsed UVI (VS25S2ZM1, Uniblitz, USA). Fluorescence was measured by an electron multiplying charge coupled device (EMCCD) (DU-897D-CS0-BV, Andor, UK, ≈−80 °C) connected to the left exit side of the microscope. To provide fluorescence simultaneous images around 450 and 590 nm, an instrument for two-channel fluorescence imaging (OptoSplit II, Andor, UK) was mounted between the EMCCD and the microscope.

2.4. Continuous and pulsed UVI

In all UVI experiments, a 100 W mercury lamp was used as the light source. Light was passed through a 365/50 nm excitation filter and focused on the sample via a Fluar 100×/1.30 oil UV objective. In the continuous UVI experiments, the erythrocytes were irradiated by the light source the entire time without the shutter. Using the EMCCD, the autofluorescence intensity data were obtained for 100 ms with a 2 s interval time. For the pulsed UVI experiments, a shutter was used to chop the continuous UV light into rectangular pulsed UV light (0.25 Hz, 1.25% duty cycle). Thus, the erythrocytes were irradiated by this pulsed UV light with an irradiation time of 50 ms with and an interval time of 4 s. Accordingly, the data for autofluorescence intensity were acquired by the EMCCD for 50 ms with a 4 s interval time.

2.5. Two-channel fluorescence imaging

Autofluorescence was measured by the imaging system discussed above. The irradiation-induced autofluorescence light was first split into two spectral channels via a dichroic mirror (562 nm edge wavelength; reflection band 425–554.5 nm; transmission band 569.5–730 nm), passed for further purification through two emission filters simultaneously (450/58 nm; 590 nm long-pass), and then simultaneously collected by the EMCCD. The images obtained were quantitatively analyzed for changes in fluorescence intensity within the region of interest using MetaMorph software version 7.1 (Universal Imaging Corp., USA).

3. Results

3.1. Exclusion of NAD(P)H autofluorescence influence in erythrocytes

It was reported that the strong autofluorescence signal in erythrocytes is due to bilirubin because the spectrums for erythrocytes and bilirubin are the same, having a signal range of 400–710 nm [14]. However, erythrocytes also contain NAD(P)H, an important endogenous fluorescent substance. Its excitation wavelength is 340 nm and the peak emission wavelength is 460 nm [16,17]. Therefore, the influence of NAD(P)H on the process of UVI-induced autofluorescence must be considered. First, in erythrocytes, a two-channel fluorescence imaging instrument was applied to detect the autofluorescence induced by continuous UV light at 9400 mW/cm^2. As illustrated in Fig. 1A, a typical two-channel autofluorescence image was obtained by the EMCCD using a 590 nm long-pass channel (left) and a 450/65 nm channel (right). Two curves were recorded simultaneously (Fig. 1B). The gray curve was obtained from the cell marked with a white ring in the left part of Fig. 1A, and the black curve was obtained from the same cell marked with a white ring in the right part of Fig. 1A. Both autofluorescence intensity curves change synchronously, indicating that NAD(P)H autofluorescence may have a negligible effect on UVI-induced autofluorescence enhancement.

To further exclude the participation of NAD(P)H from a role in the autofluorescence enhancement process, erythrocytes were pretreated with 2-DG, a nonmetabolizable analogue of glucose [18,19], and DHEA, an inhibitor of glucose-6-phosphate dehydrogenase (G6PD) [20,21], respectively. In erythrocytes, both 2-DG and G6PD can inhibit the production of NAD(P)H via the pentose phosphate pathway. The results verify that neither 2-DG nor DHEA affect the UVI-induced strong autofluorescence (data not shown). In summary, we can disregard the influence of NAD(P)H, as it had little effect on the UVI-induced autofluorescence enhancement.

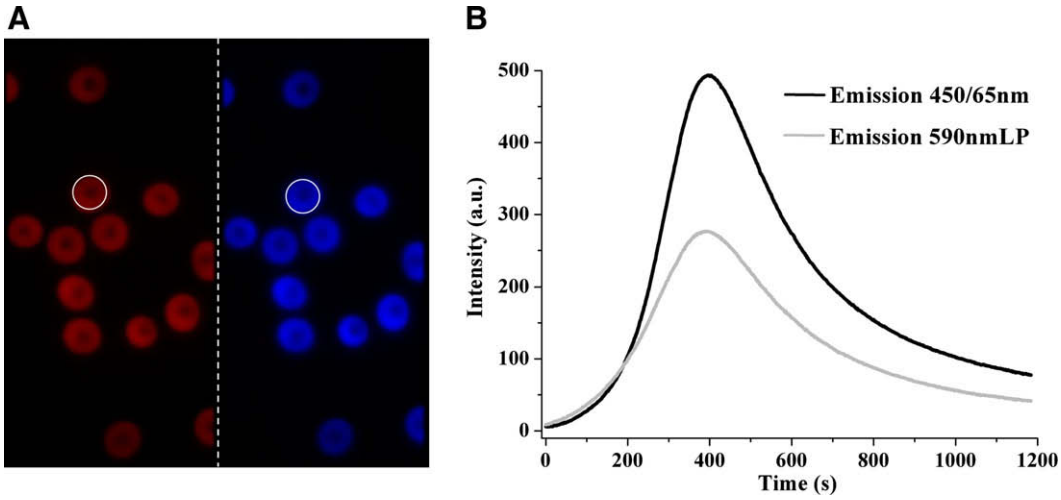

Fig. 1. Two-channel imaging of erythrocyte autofluorescence induced by continuous UVI at 9400 mW/cm^2. (A) A typical two-channel image of autofluorescence was acquired by EMCCD with a 450/65 nm emission filter (right) and a 590 nm long-pass emission filter (left). (B) Two typical curves of the erythrocyte autofluorescence intensity were recorded simultaneously. The gray curve was obtained from the autofluorescence of the cell marked with a white ring on the left side of (A), and the black line is from the autofluorescence of the circled cell on the right side of (A).

3.2. The effect of UVI on the autofluorescence in erythrocytes

In erythrocytes, we investigated the change in autofluorescence (450/58 nm emission filter) induced by a continuous and pulsed UV light at an intensity of 9400 mW/cm^2. We demonstrate that high-dose continuous UVI induces autofluorescence enhancement (black solid curve in Fig. 2A). In contrast, low-dose pulsed UVI does not have this effect on erythrocytes (gray solid curve in Fig. 2A). Moreover, we monitored the autofluorescence kinetics of erythrocytes at additional continuous UVI intensities. High-dose continuous UVI resulted in an obvious autofluorescence enhancement (black solid curve in Fig. 2B and C). While low-dose continuous UVI cannot induce an evident autofluorescence enhancement (black solid curve in Fig. 2D).

3.3. ROS accelerates UVI-induced autofluorescence enhancement in erythrocytes

It is known that ROS play a key role in various UVI-induced biological effects [7–9]. When erythrocytes were pretreated with 10 mM H_2O_2 for 5 min, UVI-induced autofluorescence data were collected using a 450/65 nm filter. As shown in Fig. 3A, the speed of the autofluorescence enhancement in H_2O_2-treated cells was much faster than that of untreated cells. Furthermore, it was found that, in the presence of H_2O_2, pulsed UVI could also induce a linear increase in autofluorescence at 9400 mW/cm^2, whereas pulsed UVI alone, at the same intensity, does not have this effect (Fig. 3B). These data indicate that ROS may have a part in the process of UVI-induced erythrocyte autofluorescence enhancement. We further demonstrated that fluorescence of a H_2O_2-pretreated hemoglobin solution could be enhanced by a low-dose continuous UVI (data not shown).

3.4. UVI-dependent autofluorescence enhancement in erythrocytes

Erythrocytes autofluorescence can be excited by not only UV light but also visible light, due to wide excitation spectrum of hemoglobin. Thus, to further determine whether this autofluorescence enhancement in erythrocytes was dependent on UVI, we irradiated cells using continuous and pulsed visible light with a 546/12 nm excitation filter. The data shows that continuous 11,800 mW/cm^2 546 nm light could only result in autofluorescence quenching, but not autofluorescence enhancement (Fig. 3C). Furthermore, when erythrocytes were pretreated with 10 mM H_2O_2 for 5 min, continuous 546 nm light was still unable to induce autofluorescence enhancement (data not shown). We also found that 11,800 mW/cm^2 pulsed 546 nm light (0.25 Hz, 1.25% duty cycle) did not cause autofluorescence enhancement in the presence of 10 mM H_2O_2 (gray line in Fig. 3D). The data clearly show that autofluorescence enhancement in erythrocytes depends on UVI. In addition, we found that fluorescence enhancement of a H_2O_2-pretreated hemoglobin solution depends on UVI (data not shown).

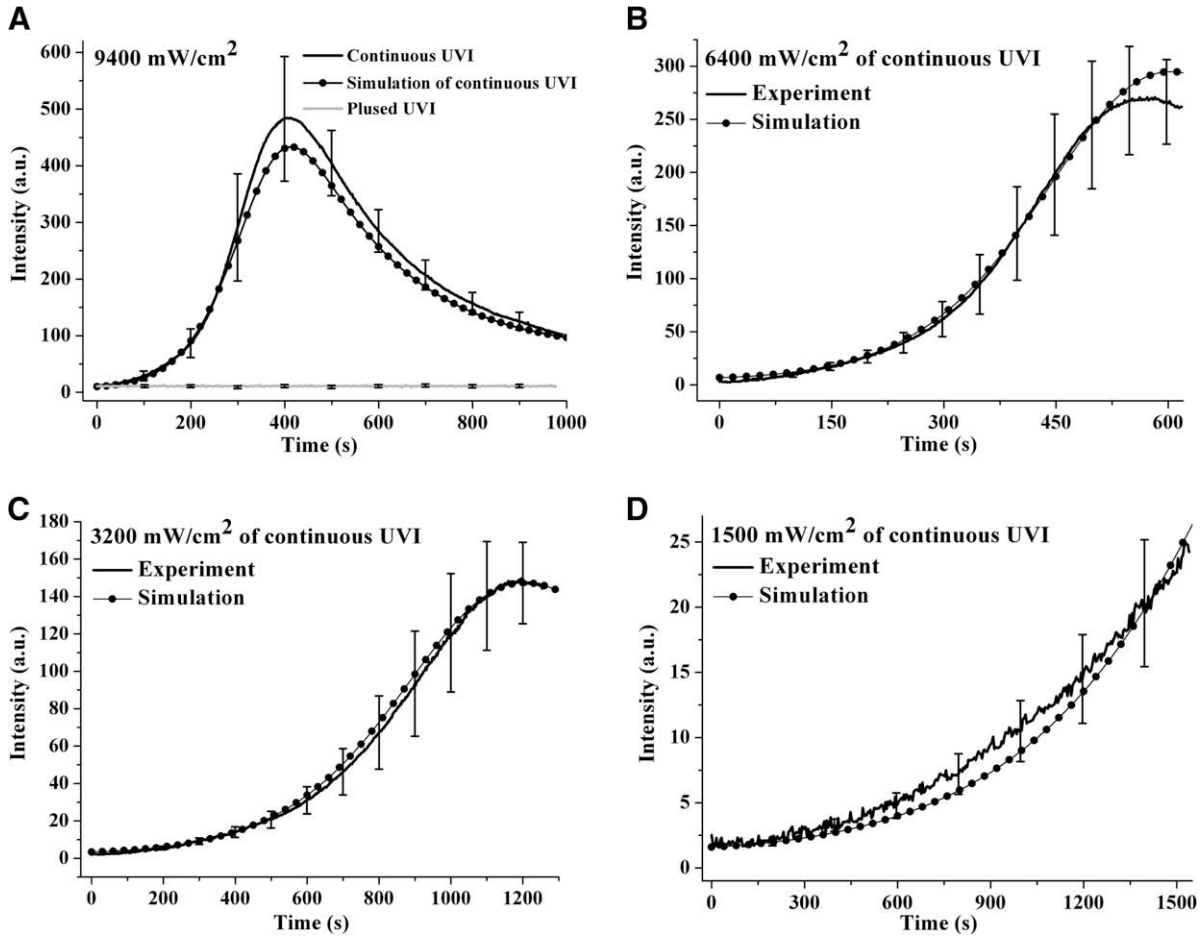

Fig. 2. Experimental (solid) and simulation (-●-) results of UVI-induced autofluorescence (450/65 nm emission filter) enhancement in erythrocytes. Experimental evolution (gray solid) of autofluorescence change induced by pulsed UVI at 9400 mW/cm^2 (A). Experimental time tracings (black solid) of autofluorescence change induced by continuous UVI at 9400 mW/cm^2 (A), 6400 mW/cm^2 (B), 3200 mW/cm^2 (C), 1500 mW/cm^2 (D). Simulation tracings (-●-) of continuous UVI-induced autofluorescence enhancement using a rate equation model at 9400 mW/cm^2 (A), 6400 mW/cm^2 (B), 3200 mW/cm^2 (C), 1500 mW/cm^2 (D). All experimental values are expressed as an averaged response from least 30 individual cells from three independent experiments.

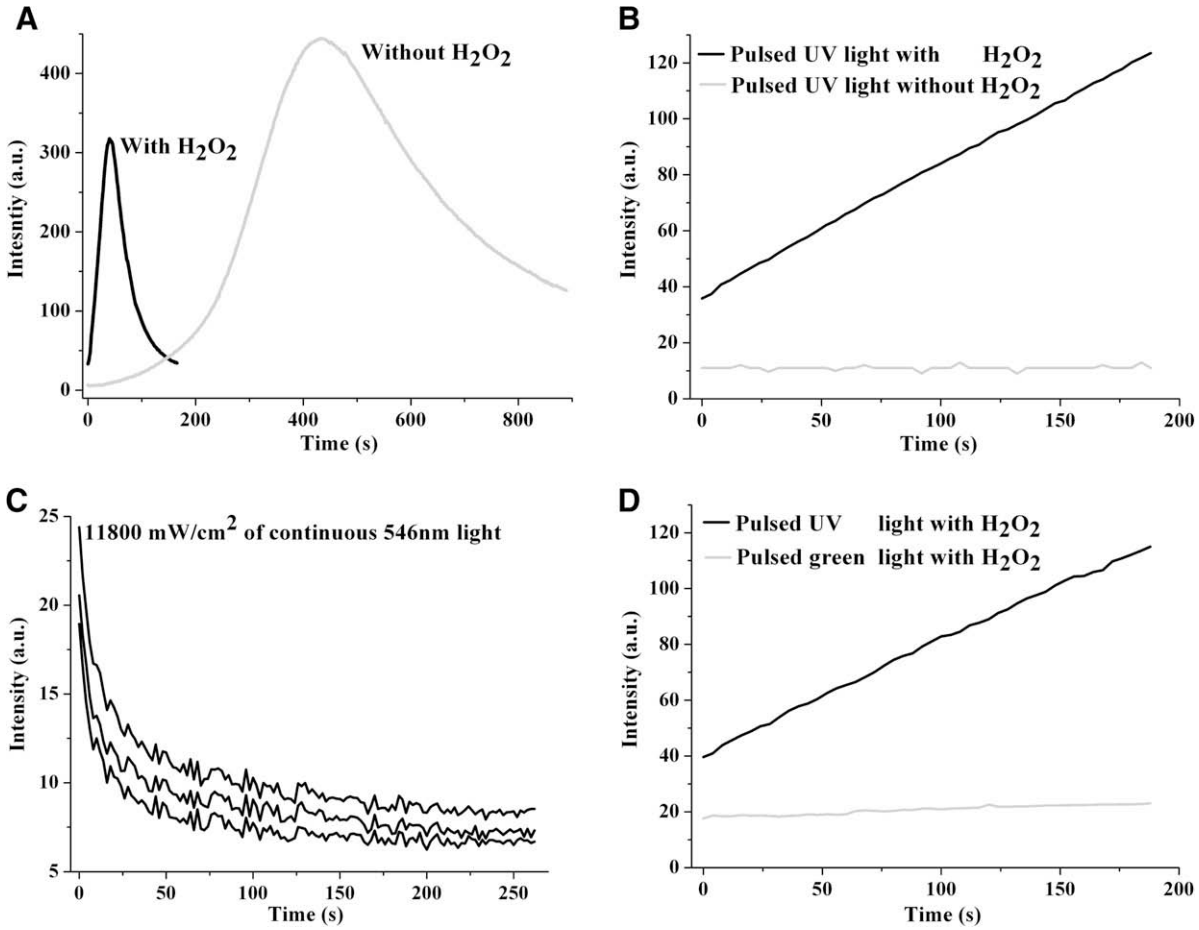

Fig. 3. H_2O_2 accelerated UVI-dependent autofluorescence enhancement in erythrocytes. (A) Typical evolutions of erythrocyte autofluorescence induced by 9400 mW/cm^2 continuous UVI in the presence or absence of 10 mM H_2O_2. (B) Representative evolutions of erythrocyte autofluorescence induced by 9400 mW/cm^2 pulsed UVI in the presence or absence of 10 mM H_2O_2. (C) Typical tracings of autofluorescence change induced by 11,800 mW/cm^2 continuous visible 546 nm light. (D) Representative tracings of autofluorescence change induced by pulsed UVI or pulsed visible 546 nm light in the presence of 10 mM H_2O_2.

4. Discussion

It is known that NAD(P)H is an important autofluorescent substance in cells, having an excitation wavelength of about 340 nm and a peak emission wavelength of 460 nm [16,17]. Many reports have shown that NAD(P)H can modulate a variety of physiological functions and signaling pathways in erythrocytes [22,23], especially in heme degradation [24]. Thus, NAD(P)H should be accounted for in the process of UVI-induced autofluorescence enhancement. First, the two-channel fluorescence imaging experiment provided direct evidence that NAD(P)H might not take part in UVI-induced autofluorescence enhancement due to the synchronous evolution of the two different fluorescence colors (Fig. 1). Second, we found no significant change in UVI-induced autofluorescence enhancement in the presence of either 2-DG or DHEA. As a nonmetabolizable analogue of glucose, 2-DG competitively antagonizes glucose utilization and greatly reduces the NAD(P)H concentration [18,19]. DHEA can also decrease the NAD(P)H level by inhibiting the G6PD activity through the pentose phosphate pathway in erythrocytes [20,21]. Given these data, we clearly demonstrate that NAD(P)H had little effect on this autofluorescence enhancement, and that its influence on autofluorescence can be neglected.

We found that only high-dose UVI from high intensity continuous irradiation can induce strong autofluorescence enhancement (Fig. 2A–C). In contrast, low-dose UVI, from either the low duty cycle of the pulsed irradiation (gray line in Fig. 2A) or a low excitation intensity (black line in Fig. 2D), did not lead to a marked autofluorescence enhancement in erythrocytes. It is well-known that high-dose UVI can produce large amounts of ROS in a variety of cell types. In addition, ROS play a key role in UV light-induced cellular physiology and pathology [7–9]. Therefore, we must consider whether ROS are involved in the UVI-induced autofluorescence enhancement process. First, it is evident that the speed of autofluorescence enhancement induced by continuous UVI was accelerated when erythrocytes were pretreated with exogenous H_2O_2 (Fig. 3A). Second, our results show that low-dose pulsed UV light could induce a linear increase in autofluorescence in the presence of H_2O_2, whereas pulsed UVI alone does not have this effect at the same irradiation intensity (Fig. 3B). These results indicate that H_2O_2 acts as a catalyst for UVI-induced autofluorescence enhancement. Taken together, we conclude that ROS is a key factor in the UVI-induced autofluorescence enhancement process, and UVI induces autofluorescence enhancement through the production of ROS in an irradiation dose-dependent manner.

Furthermore, we found that high-dose continuous visible light (546 nm) only induced autofluorescence quenching rather than enhancement (Fig. 3C), although it has been reported [25] that visible light irradiation could also produce ROS in a variety of cell types. Moreover, pulsed 546 nm light (0.25 Hz, 1.25% duty cycle) did not induce an obvious erythrocyte autofluorescence enhancement in the presence H_2O_2 (gray line in Fig. 3D). In contrast, pulsed UVI did result in autofluorescence enhancement when erythrocytes were pretreated with H_2O_2 (black line in Fig. 3B and D). Moreover, continuous 546 nm light could still not induce autofluo-

rescence enhancement when erythrocytes were pretreated with H_2O_2 (data not shown). The results also show that fluorescence enhancement of a H_2O_2-pretreated hemoglobin solution was dependent on UVI (data not shown). Considering these data, we clearly demonstrate that autofluorescence enhancement in erythrocytes depends on UVI. We propose that it is the higher single photon energy of UV light, in contrast to visible light, that leads to the photodecomposition of hemoglobin.

Given these data, we can conclude that the production of ROS and the photodecomposition of hemoglobin have two important roles in the process of UVI-induced autofluorescence enhancement in erythrocytes. With this conclusion, our next step was to try to understand the detailed mechanisms of autofluorescence enhancement induced by high-dose continuous UVI. According to our conclusions and the results of other researchers, this detailed process of autofluorescence enhancement likely occurs as follows.

When erythrocytes are irradiated by UV light, hemoglobin is elevated in energy to an excited state. This energy may be further transferred to oxygen, which induces a small production of ROS, such as superoxide and H_2O_2, due to the photodynamic effects (PDE). ROS can degrade hemoglobin or heme [26,27] and it usually reacts with hemoglobin at the heme position [28], which could cause a change in the heme ring. Therefore, we propose that exposure to UV light, due to its high single photon energy, opens the porphyrin ring of heme. Aided by ROS, this UV exposure releases heme iron and yields bilirubin, which has a high fluorescence efficiency. Notably, there is a one-to-one relationship between heme and bilirubin. Thus, it is actually the formation of bilirubin that leads to autofluorescence enhancement due to the high fluorescence efficiency of bilirubin. Moreover, bilirubin, an efficient photosensitizer [14], can further form much more ROS. As the degradation rate of hemoglobin or heme depends on the ROS concentration [26], much more bilirubin are produced, thus, a rapid increase in autofluorescence enhancement was observed (black solid curve in Fig. 2A). Because continuous UV light can induce photodegradation of bilirubin [29], ROS are also involved in the degradation of bilirubin [30], and the amount of hemoglobin is limited in erythrocytes, it seems obvious that the autofluorescence will decrease when the formation rate of bilirubin is slower than the photodegradation rate (black solid curve in Fig. 2A). However, even after a long period of continuous irradiation, the autofluorescence decline does not decline to the initial level, indicating that the photodegradation products of bilirubin might still have some fluorescence efficiency. Furthermore, we can speculate that the fluorescence efficiency of bilirubin photodegradation products may be lower than that of intact bilirubin, but higher than that of hemoglobin, where there is a one-to-one relationship between bilirubin and its photodegradation products. Taken together, the

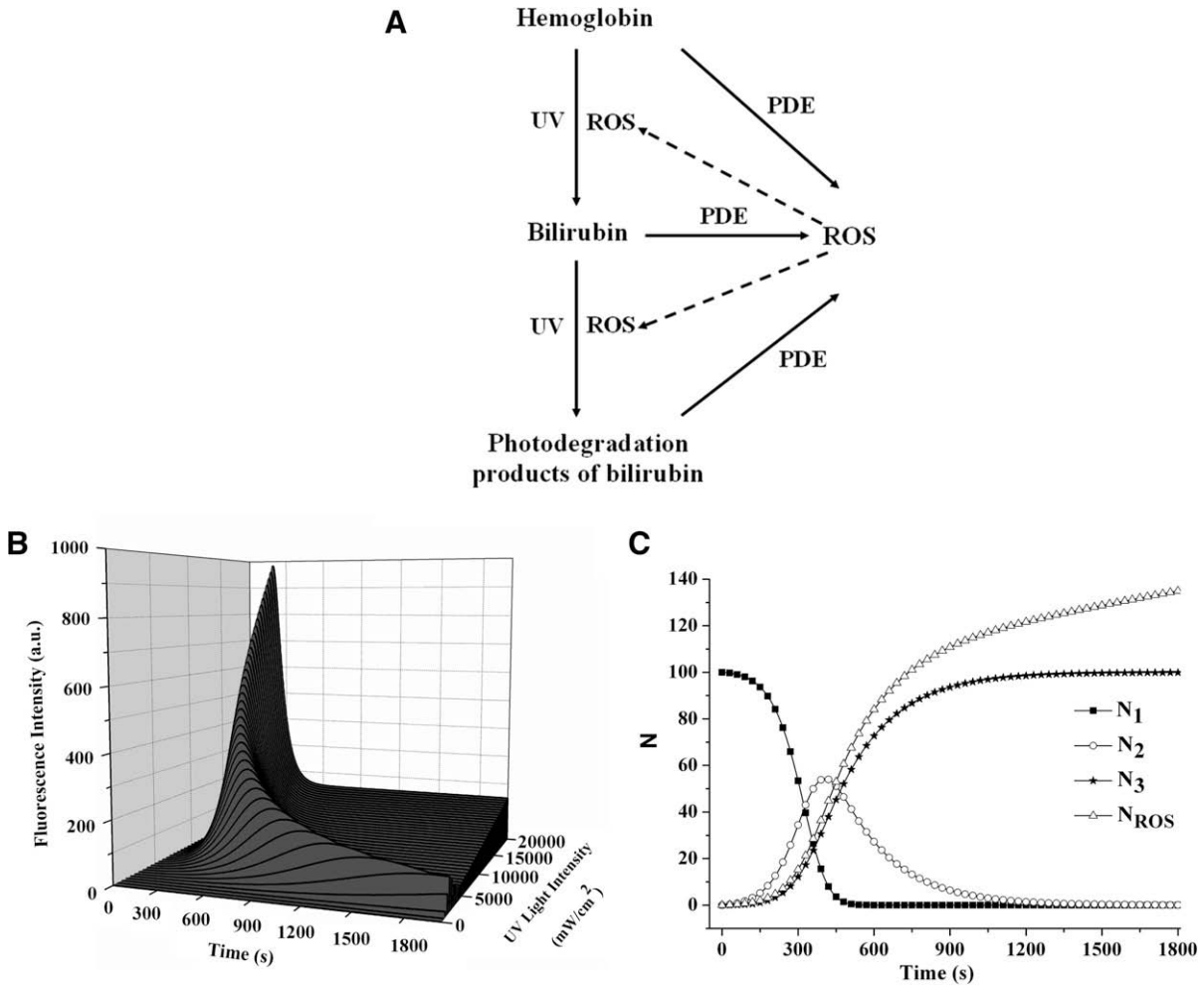

Fig. 4. Theoretical simulation of continuous UVI-induced autofluorescence enhancement the process using a rate equation. (A) Schematic representation of the proposed reaction pathway for UVI-induced autofluorescence enhancement. Dashed arrows indicate that the ROS produced by PDE are involved in degradation of hemoglobin and bilirubin. (B) The simulation time tracings of autofluorescence enhancement using different UVI intensities. (C) Population density time evolutions of hemoglobin (N_1, ■), bilirubin (N_2, ○), photodegradation products of bilirubin (N_3, *), and ROS (N_{ROS}, △) at a UVI intensity of 9400 mW/cm^2.

proposed reaction pathways for high-dose continuous UVI-induced autofluorescence enhancement are schematically summarized in schematic form, Fig. 4A.

According our suggested continuous UV light-induced autofluorescence enhancement process, we further simulated this process using a rate equation model. The rate equation system is as follows:

$$\begin{aligned}
\frac{\partial N_1}{\partial t} &= -\gamma(N_{ROS}, I_0)N_1 \approx (-\gamma_0 N_1 - \gamma_1 N_{ROS} N_1)C_1 I_0 \\
\frac{\partial N_2}{\partial t} &= \gamma(N_{ROS}, I_0)N_1 - \beta(N_{ROS}, I_0)N_2 \\
&\approx (\gamma_0 N_1 + \gamma_1 N_{ROS} N_1)C_1 I_0 - (\beta_0 N_2 + \beta_1 N_{ROS} N_2)C_2 I_0 \qquad (1) \\
\frac{\partial N_3}{\partial t} &= \beta(N_{ROS}, I_0)N_2 \approx (\beta_0 N_2 + \beta_1 N_{ROS} N_2)C_2 I_0 \\
\frac{\partial N_{ROS}}{\partial t} &= (\sigma_1 N_1 + \sigma_2 N_2 + \sigma_3 N_3)C_3 I_0 \\
N_1 + N_2 + N_3 &= N_0
\end{aligned}$$

Eq. (1) can be explained as follows: N_1 is the population density of heme (N_1 is four times larger than that of hemoglobin), N_2 is the population density of bilirubin, and N_3 is the population density of the bilirubin photodegradation products. The initial value of N_1 is N_0 ($t = 0$) and the initial value of N_2 and N_3 are zero ($t = 0$). There is a one-to-one relationship among N_1, N_2 and N_3. N_{ROS} is the population density of ROS. $\gamma(N_{ROS}, I_0)$ and $\beta(N_{ROS}, I_0)$ are coefficients of the photodecomposition speed. First, the influence of ROS is taken into consideration because we have concluded that the production of ROS is a key factor in UVI-induced autofluorescence enhancement. It is reported that the ROS are involved in degradation processes of hemoglobin [26] and bilirubin [30]. Second, the intensity of the UVI should be taken into consideration because our data showed that the different intensities of UVI also have different effects on the autofluorescence enhancement (Fig. 2). Therefore, for convenience in our calculations, we propose that both ROS and UVI intensities induce a simple linear effect on γ and β. C_1, C_2, and C_3 are coefficients related to I_0. In addition, ROS can be formed from heme, bilirubin and photodegradation products of bilirubin due to the PDE. Thus, σ_1, σ_2 and σ_3 are the coefficients of the ROS production speed.

Therefore, the autofluorescence intensity FI can be expressed as follows:

$$FI = kI_0(\Phi_1 N_1 + \Phi_2 N_2 + \Phi_3 N_3) \qquad (2)$$

Here Φ_1 is the fluorescence efficiency of hemoglobin, Φ_2 is the fluorescence efficiency of bilirubin, and Φ_3 is the fluorescence efficiency of the photodegradation products of bilirubin. To test the accuracy of this theoretical simulation, model parameter values were chosen according to the experiments, which are $N_0 = 100$, $\gamma_0 = 1/16{,}000$, $\gamma_1 = 1/1850$, $\beta_0 = 1/230$, $\beta_1 = 1/200{,}000$, $C_1 = C_2 = C_3 = 1/9400$, $\sigma_1 = 1/20{,}000$, $\sigma_2 = 1/200$, $\sigma_3 = 1/5000$, $\Phi_1 = 0.01$, $\Phi_2 = 0.75$, $\Phi_3 = 0.07$, and $k = 1/940$. Finally, we obtained a theoretical evolution curve of FI using numerical simulation. Fig. 4B illustrates the simulation of the autofluorescence evolution at the different UVI intensities. We found that the results of the theoretical simulation are in accordance with the experimental data at different UV light intensities, 9400, 6400, 3200 and 1500 mW/cm^2 (-●- curves in Fig. 2). Furthermore, we can predict the evolutions of N_1, N_2, N_3 and N_{ROS} using this rate equation model, as such evolutions can be difficult to obtain from experiments. Fig. 4C shows the simulation tracings for N_1, N_2, N_3 and N_{ROS} evolutions at a UVI intensity of 9400 mW/cm^2.

Although this theoretical simulation using the rate equation model is in accordance with the experiments, other influences should still be considered, including fluorescence quenching, nonlinear effects on $\gamma(N_{ROS}, I_0)$ and $\beta(N_{ROS}, I_0)$, and other sources of ROS. Moreover, if we can determine experimental values of certain parameters, the empirical parameters may increase the accuracy of rate equation model. Given these data, the rate equation model can qualitatively provide some explanation as to the mechanisms underlying continuous UVI-induced autofluorescence enhancement. This simulation further supports our conclusions that UVI plays two roles in the autofluorescence enhancement process.

In conclusion, our data clearly show that continuous UVI induces autofluorescence enhancement of erythrocytes in an irradiation dose-dependent manner. We found that NAD(P)H has little effect on this autofluorescence enhancement. Furthermore, we conclude that the production of ROS and UVI-dependent photodecomposition play two important roles in the process of UVI-induced autofluorescence enhancement. Finally, we successfully simulated this UVI-induced autofluorescence enhancement process using a rate equation model. As erythrocytes often serve as model cells for PDT, we believe that this study on UVI-induced autofluorescence enhancement might fill an important gap in the research on PDT in erythrocytes.

Acknowledgments

This work was supported by the National Basic Research Program of China (2007CB307002, 2010CB934101) and 111 Project (No. B07013).

References

[1] W. Silny, A. Osmola-Mankowska, M. Czarnecka-Operacz, R. Żaba, A. Danczak-Pazdrowska, A. Marciniak, Eosinophilic fascitis: a report of two cases treated with ultraviolet A1 phototherapy, Photodermatol. Photoimmunol. Photomed. 25 (2009) 325–327.
[2] P. Chandra, L.L. Wolfenden, T.R. Ziegler, J. Tian, M. Luo, A.A. Stecenko, T. Chen, M.F. Holick, V. Tangpricha, Treatment of vitamin D deficiency with UV light in patients with malabsorption syndromes: a case series, Photodermatol. Photoimmunol. Photomed. 23 (2007) 179–185.
[3] R.P. Gallaghera, T.K. Lee, Adverse effects of ultraviolet radiation: a brief review, Prog. Biophys. Mol. Biol. 92 (2006) 119–131.
[4] M.R. Hussein, Ultraviolet radiation and skin cancer: molecular mechanisms, J. Cutan. Pathol. 32 (2005) 191–205.
[5] A.R. Young, Acute effects of UVR on human eyes and skin, Prog. Biophys. Mol. Biol. 92 (2006) 80–85.
[6] A.M. Moodycliffe, D. Nghiem, G. Clydesdale, Immune suppression and skin cancer development: regulation by NKT cells, Nat. Immunol. 1 (2000) 521–525.
[7] K. Scharffetter-Kochanek, M. Wlaschek, P. Brenneisen, M. Schauen, R. Blaudschun, J. Wenk, UV-induced reactive oxygen species in photocarcinogenesis and photoaging, Biol. Chem. 378 (1997) 1247–1257.
[8] A. Valenciaa, I.E. Kochevar, Ultraviolet A induces apoptosis via reactive oxygen species in a model for Smith–Lemli–Opitz syndrome, Free Radic. Biol. Med. 40 (2006) 641–650.
[9] C.L. Hsieh, G.C. Yen, H.Y. Chen, Antioxidant activities of phenolic acids on ultraviolet radiation-induced erythrocyte and low density lipoprotein oxidation, J. Agric. Food Chem. 53 (2005) 6151–6155.
[10] A.L.Y. Lecluse, V.C.M. Kuck-Koot, H. van Weelden, V. Sigurdsson1, I.M. Russel, J. Frank, S.G.M.A. Pasmans, Erythropoietic protoporphyria without skin symptoms – you do not always see what they feel, Eur. J. Pediatr. 167 (2008) 703–706.
[11] Y. He, D.C. Ramirez, C.D. Detweiler, R.P. Mason, C.F. Chignell, UVA-ketoprofen-induced hemoglobin radicals detected by immuno-spin trapping, Photochem. Photobiol. 77 (2003) 585–591.
[12] I.E. Kochevar, UV-induced protein alterations and lipid oxidation in erythrocyte membranes, Photochem. Photobiol. 52 (1990) 795–800.
[13] R.B. Misra, R.S. Ray, R.K. Hans, Effect of UVB radiation on human erythrocytes in vitro, Toxicol. In Vitro 19 (2005) 433–438.
[14] L. Kaestner, A. Juzeniene, J. Moan, Erythrocytes – the house elves of photodynamic therapy, Photochem. Photobiol. Sci. 3 (2004) 981–989.
[15] L. Kaestner, W. Tabellion, E. Weiss, I. Bernhardt, P. Lipp, Calcium imaging of individual erythrocytes: problems and approaches, Cell Calcium 39 (2006) 13–19.
[16] L. Pan, X. Zhang, K. Song, W. Cai, X. Wu, R. Rupp, J. Xu, Real-time imaging of autofluorescence NAD(P)H in single human neutrophils, Appl. Opt. 48 (2009) 1042–1046.
[17] W. Ying, NAD+/NADH and NADP+/NADPH in cellular functions and cell death: regulation and biological consequences, Antioxid. Redox Signal. 10 (2008) 179–206.
[18] C.E. Stafstrom, A. Roopra, T.P. Sutula, Seizure suppression via glycolysis inhibition with 2-deoxy-D-glucose (2DG), Epilepsia 49 (2008) 97–100.
[19] L. Pan, X. Zhang, K. Song, X. Wu, J. Xu, Exogenous nitric oxide-induced release of calcium from intracellular IP_3 receptor-sensitive stores via S-nitrosylation in

respiratory burst-dependent neutrophils, Biochem. Biophys. Res. Commun. 377 (2008) 1320–1325.
[20] W.N. Tian, L.D. Braunstein, J. Pang, K.M. Stuhlmeier, Q.C. Xi, X. Tian, R.C. Stanton, Importance of glucose-6-phosphate dehydrogenase activity for cell growth, J. Biol. Chem. 273 (1998) 10609–10617.
[21] E.S. Shin, J. Park, J.M. Shin, D. Cho, S.Y. Cho, D.W. Shin, M. Ham, J.B. Kim, T.R. Lee, Catechin gallates are $NADP^+$-competitive inhibitors of glucose-6-phosphate dehydrogenase and other enzymes that employ $NADP^+$ as a coenzyme, Bioorg. Med. Chem. 16 (2008) 3580–3586.
[22] R.A. Olek, J. Antosiewicz, G.C. Caulini, G. Falcioni, Effect of NADH on the redox state of human hemoglobin, Clin. Chim. Acta 324 (2008) 129–134.
[23] M. Vetrella, B. Astedt, W. Barthelmai, D. Neuvians, Activity of NADH- and NADPH-dependent methemoglobin reductases in erythrocytes from fetal to adult age, J. Mol. Med. 49 (1970) 1432–1440.
[24] T. Yoshida, Heme oxygenase and heme degradation, Seikagaku 75 (2003) 204–212.
[25] R. Lavi, A. Shainberg, H. Friedmann, V. Shneyvays, O. Rickover, M. Eichler, D. Kaplan, R.L. Lubart, Low energy visible light induces reactive oxygen species generation and stimulates an increase of intracellular calcium concentration in cardiac cells, J. Biol. Chem. 278 (2003) 40917–40922.
[26] E. Nagababu, F.J. Chrest, J.M. Rifkind, Hydrogen-peroxide-induced heme degradation in red blood cells: the protective roles of catalase and glutathione peroxidase, Biochim. Biophys. Acta 1620 (2003) 211–217.
[27] E. Nagababu, J.M. Rifkind, Formation of fluorescent heme degradation products during the oxidation of hemoglobin by hydrogen peroxide, Biochem. Biophys. Res. Commun. 247 (1998) 592–596.
[28] J. Zhao, W. Meng, P. Miao, Z. Yu, G. Li, Photodynamic effect of hypericin on the conformation and catalytic activity of hemoglobin, Int. J. Mol. Sci. 9 (2008) 145–153.
[29] A.F. McDonagh, The role of singlet oxygen in bilirubin photo-oxidation, Biochem. Biophys. Res. Commun. 44 (1971) 1306–1311.
[30] R. Kaul, H. Kaul, P. Bajpai, C. Murti, Evidence for the possible involvement of the superoxide radicals in the photodegradation of bilirubin, J. Biosci. 1 (1979) 377–383.